JACS
JOURNAL OF THE AMERICAN CHEMICAL SOCIETY

ARTICLE

pubs.acs.org/JACS

Photochemistry of 2-Naphthoyl Azide. An Ultrafast Time-Resolved UV–Vis and IR Spectroscopic and Computational Study

Jacek Kubicki,[†] Yunlong Zhang,[‡] Shubham Vyas,[‡] Gotard Burdzinski,[†] Hoi Ling Luk,[‡] Jin Wang,[‡,#] Jiadan Xue,[‡] Huo-Lei Peng,[‡] Elena A. Pritchina,[⊥] Michel Sliwa,[§] Guy Buntinx,[§] Nina P. Gritsan,[⊥] Christopher M. Hadad,*[,‡] and Matthew S. Platz*[,‡]

[†]Quantum Electronics Laboratory, Faculty of Physics, Adam Mickiewicz University, Umultowska 85, 61-614 Poznań, Poland

[‡]Department of Chemistry, The Ohio State University, 100 West 18th Avenue, Columbus, Ohio, 43210, United States

[§]Laboratoire de Spectrochimie Infrarouge et Raman (LASIR), UMR 8516/CNRS –Université Lille 1 Sciences et Technologies, 59655 Villeneuve d'Ascq, France

[⊥]Institute of Chemical Kinetics and Combustion, Siberian Branch of Russian Academy of Science and Novosibirsk State University, 630090 Novosibirsk, Russia

Ⓢ *Supporting Information*

ABSTRACT: The photochemistry of 2-naphthoyl azide was studied in various solvents by femtosecond time-resolved transient absorption spectroscopy with IR and UV–vis detection. The experimental findings were interpreted with the aid of computational studies. Using polar and nonpolar solvents, the formation and decay of the first singlet excited state (S_1) was observed by both time-resolved techniques. Three processes are involved in the decay of the S_1 excited state of 2-naphthoyl azide: intersystem crossing, singlet nitrene formation, and isocyanate formation. The lifetime of the S_1 state decreases significantly as the solvent polarity increases. In all solvents studied, isocyanate formation correlates with the decay of the azide S_1 state. Nitrene formation correlates with the decay of the relaxed S_1 state only upon 350 nm excitation ($S_0 \rightarrow S_1$ excitation). When S_n ($n \geq 2$) states are populated upon excitation (λ_{ex} = 270 nm), most nitrene formation takes place within a few picoseconds through the hot S_1 and higher singlet excited states (S_n) of 2-naphthoyl azide. The data correlate with the results of electron density difference calculations that predict nitrene formation from the higher-energy singlet excited states, in addition to the S_1 state. For all of these experiments, no recovery of the ground state was observed up to 3 ns after photolysis, which indicates that both internal conversion and fluorescence have very low efficiencies.

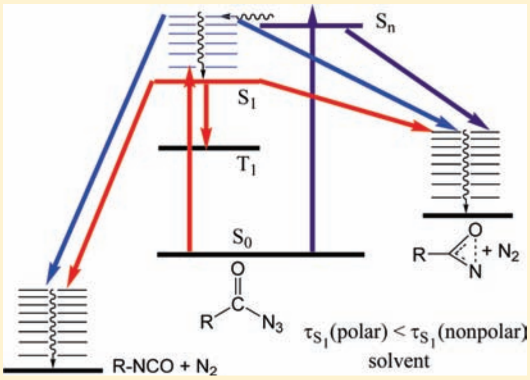

1. INTRODUCTION

The Curtius rearrangement can be initiated with either light or heat.[1,2] Irradiation of acyl azides in solution produces two primary photoproducts: isocyanate (photo-Curtius rearrangement) and nitrene.[1,2]

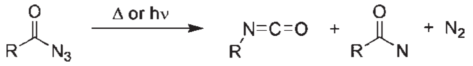

$$RC(O)N_3 \xrightarrow{\Delta \text{ or } h\nu} RN{=}C{=}O + RC(O)N + N_2$$

As singlet nitrenes are very reactive species, azides are often used as photoaffinity labels.[3] It is well-known that alkyl- and arylnitrenes have triplet ground states,[2,4] although aroylnitrenes have singlet ground states.[1,2,5–9] Theory predicts that the CON moiety in the singlet ground state of formyl-, acetyl-, benzoyl-, and naphthoyl-nitrenes have geometries that are intermediate between an idealized trigonal planar geometry and cyclic oxazirine.[5,6,9] Nevertheless, singlet carbonyl nitrenes do follow traditional nitrene reactions, such as insertion into C–H bonds and addition to C═C bonds.[1,2,9] The N···O bonding interaction explains why the closed-shell singlet states of aroylnitrenes are more stable than the corresponding triplet isomers.[5,6,9] Similar effects have been noted for phosphorylnitrenes.[10] As isocyanate formation competes with nitrene formation, the efficiency of acyl azides as photoaffinity labels is reduced. On the other hand, isocyanates are important monomers in polyurethane synthesis and are easily produced by Curtius rearrangement.[11] Recently, it was shown that a cyanate product is also formed upon carbonyl azide decomposition but in very low yield relative to the isocyanate isomer (~1%).[12]

Received: October 10, 2010
Published: May 09, 2011

Thermal Curtius rearrangement of various acyl azides are well-known,[13−15] and this process is a concerted reaction of azides, which bypasses nitrene intermediates.[1,9,15,16] Thermolysis of pivaloyl azide in cyclohexane does not generate a trappable nitrene in more than minute quantities and instead produces isocyanate in nearly quantitative yield.[15] On the contrary, photolysis of pivaloyl azide gives isocyanate only in 40% yield as well as products derived from interception of a nitrene intermediate.[13,14] Photolysis of benzoyl azide and a series of its derivatives afforded isocyanates in similar yields (40−50%) along with adducts derived from nitrenes.[17,18] Therefore, carbonylnitrenes are clearly produced upon photolysis of carbonyl azides, in contrast to their thermolysis.

The photochemical Curtius rearrangement is a concerted reaction to form the isocyanate product and does not involve either thermally relaxed nitrenes[5] or hot nitrenes.[19] We view this as an example of a "Rearrangement in the Excited State" (an RIES[20]) mechanism.

The photochemistry of benzoyl azide was previously studied by nanosecond time-resolved infrared (ns TRIR) spectroscopy.[5] In this seminal study, the formation of isocyanate and nitrene products could not be resolved with the experimental time resolution available (50 ns) at that time. These experiments did demonstrate, however, that benzoylnitrene, in the ground state, does not isomerize to isocyanate in solution under conditions typical of laser flash photolysis studies.

Xanthone-sensitized ns TRIR experiments[21] demonstrated that an excited singlet state of benzoyl azide must be the precursor of phenyl isocyanate, consistent with the earlier findings of Schuster and co-workers with substituted aroyl azides containing internal sensitizers.[7] Similar conclusions were drawn by Toscano et al. in a related study of the photochemistry of *N*-benzoyl and *N*-acetyl dibenzothiophene sulfilimines with ns TRIR techniques.[21,22]

Triplet-sensitized photolysis of 2-naphthoyl azide (2-$NpCON_3$) in cyclohexane produces only a very small amount of isocyanate (5%) as compared to direct excitation of 2-$NpCON_3$ (~58%).[8] It was concluded that the isocyanate formed upon triplet sensitization was produced by inadvertent direct irradiation of 2-$NpCON_3$. Thus, an excited singlet state of the acyl azide is the likely precursor of the isocyanate. However, this hypothesis has never been confirmed by direct correlation of the decay of the excited singlet state of the acyl azide with the corresponding growth of the isocyanate. To test this hypothesis, we sought unique vibrational marker bands for all of the relevant species using femtosecond TRIR spectroscopy. Marker bands in the IR region can allow independent monitoring of the dynamics of different species in cases where their electronic spectra may significantly overlap. Fortunately, the NCO vibration of the isocyanate moiety is IR active and its intensity is large. The singlet excited states of acyl azides have prominent IR bands as well.[19] Recently, we reported observation of the decay of the S_1 state of an aryldiazirine and the formation of its isomeric diazo compound and related singlet carbene using this approach.[23]

The photochemistry of 2-$NpCON_3$ has been studied extensively,[7,8] but the dynamics of isocyanate and nitrene formation were not previously determined. In our preliminary report, the photochemistry of benzoyl azide ($PhCON_3$), 2-naphthoyl azide (2-$NpCON_3$), and pivalolyl azide (t-$BuCON_3$) was examined in chloroform at ambient temperature solely by means of femtosecond (fs) TRIR spectroscopy.[19] We reported that the first singlet excited states of the acyl azides are the precursors of the corresponding isocyanate products.[19] The lifetime of the S_1 state of 2-$NpCON_3$ was found to be about 120 ps,[19] consistent with Autrey and Schuster's findings (<2 ns).[8] 2-$NpCON_3$ has a convenient chromophore for UV−vis studies, and intense IR markers. Thus, we were encouraged to study the photochemistry of 2-$NpCON_3$ in different solvents using both the fs TRIR and fs UV−vis transient absorption techniques, as well as with modern quantum chemical calculations.

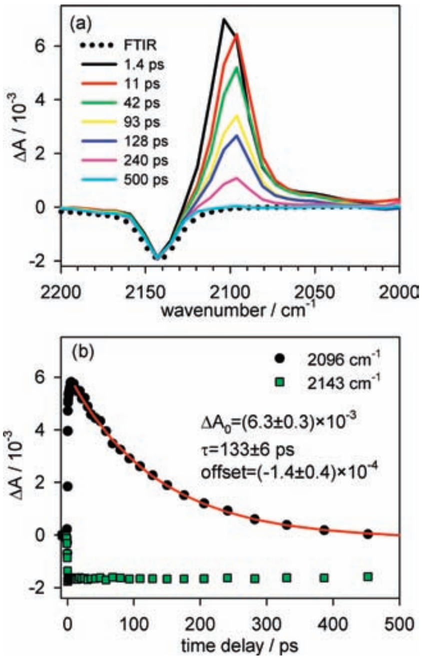

Figure 1. (a) TRIR spectra produced upon 350 nm excitation of 2-$NpCON_3$ (c ~ 4.0 × 10^{-3} M) in chloroform. The normalized steady-state IR absorption spectrum (FTIR) of 2-$NpCON_3$ in chloroform is shown as a dotted line. (b) The decay of the S_1 state recorded at 2096 cm^{-1}, and the kinetics of the signal at 2143 cm^{-1} (the depopulation band of the ground state).

2. EXPERIMENTAL RESULTS

2.1. Ultrafast IR and UV−Vis Studies of the Photochemistry of 2-Naphthoyl Azide with 350 nm Excitation.

Ultrafast IR Studies. Figure 1 and Figure S2 (see Supporting Information) present the IR transient absorption spectra produced upon 350 nm excitation of 2-$NpCON_3$ in selected solvents. Analysis of the electronic absorption spectrum of 2-$NpCON_3$ (Figure S3, Supporting Information) and time-dependent B3LYP (TD-B3LYP) calculations predict that 350 nm light directly populates the S_1 state (vide infra, Table S7, Supporting Information). In all solvents employed, photoexcitation of 2-$NpCON_3$ generates a transient 2100 cm^{-1} band, which is formed within the laser pulse (300 fs, Figure S4, Supporting Information). This band was assigned previously to the S_1 state of 2-$NpCON_3$.[19] This assignment is supported by theory (vide infra). Indeed, calculations predict that the vibrational frequency of the N_3 stretch in the S_1 state of 2-$NpCON_3$ is lower by 72 cm^{-1} and its intensity is higher by about a factor of 3, relative to the S_0 state (Figure S5, Table S2, Supporting Information).

The decay of the 2100 cm^{-1} band can be adequately fit to a monoexponential decay upon 350 nm excitation in all solvents used in this study (Figure 1 and Figure S2). The lifetimes of the S_1 state of 2-$NpCON_3$, determined using the fs TRIR transient absorption technique, are presented in Table 1. This table also

Table 1. Solvent Properties and Time Constants (τ) Describing the Decay of the Excited S_1 State of 2-NpCON$_3$ Obtained from fs TRIR and fs UV−Vis Spectroscopic Detection

		decay of the S_1 state		
solvent	f(ε,n)[a]	initially excited state	τ (ps) IR detection 2100 cm^{-1}	τ (ps) UV−vis detection 350−650 nm
cyclohexane	−0.0007	S_n[b]	14.0 ± 1.6,[c] 580 ± 60 [d]	–
		S_1[e]	800 ± 120 [d,e]	–
carbon tetrachloride	0.0116	S_n[b]	8.6 ± 0.8,[c] 570 ± 50 [d]	–
		S_1[e]	690 ± 60 [d,e]	425 ± 12 [d,e]
chloroform	0.1550	S_n[b]	6.8 ± 1.3,[c,f] 120 ± 30 [d,f]	6 ± 2, [c] 130 ± 20 [d]
		S_1[e]	133 ± 6 [d,e]	–
dichloromethane	0.2305	S_n[b]	6.5 ± 1.1,[c] 70 ± 6 [d]	–
acetonitrile	0.3303	S_n[b]	3.0 ± 0.7,[c] 19 ± 4 [d]	3 ± 1, [c] 23 ± 4 [d]
		S_1[e]	28 ± 5 [d,e]	26 ± 4 [d,e]
methanol	0.3327	S_n[b]	3.6 ± 0.9,[c] 19 ± 3 [d]	2.0 ± 0.2,[c] 24 ± 3 [d]

[a] $f(\varepsilon,n) = (\varepsilon - 1)/(2\varepsilon + 1) - (n^2 - 1)/(2n^2 + 1)$: n = refractive index, ε = dielectric constant.[24] [b] 270 nm excitation was used to populate S_n ($n > 1$) excited states. With this excitation wavelength, biexponential decays were observed. [c] Vibrational cooling (VC) and Curtius rearrangement of the hot S_1. [d] Decay of vibrationally relaxed S_1 state. [e] When 340 or 350 nm excitation was used, a monoexponential decay of S_1 was observed. [f] τ in chloroform was taken from ref 19.

Table 2. The Efficiency of Isocyanate (Φ_{NCO}), Nitrene ($\Phi_{nitrene}$), and Triplet Azide (Φ_T) Formation and the Corresponding Rate Constants in Three Selected Solvents

solvent	Φ_{NCO}[a]	k_{NCO}[b] (× 10^9 s^{-1})	Φ_T[e]	k_{ISC}[f] (× 10^9 s^{-1})	$\Phi_{nitrene}$[c]	$k_{nitrene}$[d] (× 10^9 s^{-1})
CH_2Cl_2	0.67 ± 0.11	9.6 ± 2.4	0.020 ± 0.005	0.29 ± 0.10	0.31 ± 0.06	4.4 ± 1.2
$CHCl_3$	0.62 ± 0.09	5.2 ± 0.9	0.04 ± 0.01	0.31 ± 0.09	0.34 ± 0.05	2.8 ± 0.5
CCl_4	0.52 ± 0.09	0.75 ± 0.20	0.29 ± 0.06	0.51 ± 0.15	0.19 ± 0.03	0.28 ± 0.07

[a] $\Phi_{NCO} = |A_{NCO}/A_{N_3}| \times (\varepsilon N_3/\varepsilon NCO)$. [b] $k_{NCO} = \Phi_{NCO} \times \tau^{-1}$, τ the lifetime of the S_1 state taken from Table 1. [c] $\Phi_{nitrene} = 1 - (\Phi_{NCO} + \Phi_T)$. [d] $k_{nitrene} = \Phi_{nitrene} \times \tau^{-1}$. [e] Taken from Table S1. [f] $k_{ISC} = \Phi_T \times \tau^{-1}$.

presents the time constants measured using fs UV−vis transient absorption spectroscopy. In the latter case, the decay of the S_1 absorption band of 2-NpCON$_3$ was analyzed (vide infra). In addition, Table 1 includes the time constants obtained when 270 nm excitation was used, and thus higher excited states were initially populated (vide infra).

A small shift of the maximum of the IR band of the 2-NpCON$_3$ S_1 state to lower frequency was observed during the first 5 ps in chloroform. This effect was attributed to the dynamics of solvation[25] (Figure S6, Supporting Information). This interpretation is in agreement with the computational prediction that the dipole moment of 2-NpCON$_3$ increases significantly upon excitation, from 3.8 D in the S_0 state to 11.3 D in the S_1 (π,π*) state.

As the S_1 state is very polar, one might reasonably expect, applying ground-state reasoning, that it would be kinetically stabilized in polar solvents, yet the trend in lifetime is in the opposite direction. Of course, the solvent effect is difficult to interpret because the decay of the S_1 state is controlled by several solvent-dependent processes including isocyanate formation, nitrene formation, and triplet formation and the rate of each process will respond differently to solvent variation.

The amplitude of the N$_3$ bleach of 2-NpCON$_3$ at about 2140 cm^{-1} does not change over 3 ns (Figures 1 and S2). Thus, in all of the solvents utilized in this study, there is no recovery of the ground state on this time scale. This means that both internal conversion (IC, $S_1 \rightarrow S_0$) and fluorescence have small quantum yields. In our opinion, the large energy gap between the S_1 and S_0 states (~85 kcal/mol, see Table S7) plays a key role in lowering the rate constant and thus, the efficiency of IC.

To better understand the influence of solvent, the efficiency of isocyanate formation was estimated in solvents with different polarities (CCl_4, $CHCl_3$, CH_2Cl_2). These solvents are relatively transparent to IR light (1 mm layer of solution) in the spectral range where an isocyanate has a strong IR marker. In these experiments, the S_1 state was directly populated using 340 nm excitation. The experimental IR difference spectra were recorded, and the amplitudes of the isocyanate (A_{NCO}) and azide (A_{N3}) bands were compared in different solvents (Figure S7, Supporting Information). The extinction coefficients for the NCO vibration (ε_{NCO}) in these solvents were determined with an authentic sample of 2-NpNCO and the extinction coefficients for the N$_3$ vibration (ε_{N_3}) for 2-NpCON$_3$ were determined as well (Table S3, Supporting Information). Using values of ε_{NCO} and ε_{N_3} we estimated the efficiency (Φ_{NCO}) and the rate constant ($k_{NCO} = \Phi_{NCO} \times \tau^{-1}$) of isocyanate formation in different solvents (Table 2). In the most polar solvent employed, CH_2Cl_2, the rate constant and efficiency of isocyanate formation are the largest among the three solvents used. The ratios of the rate constants of isocyanate formation were estimated to be about 1:7:13 in CCl_4, $CHCl_3$, and CH_2Cl_2, respectively.

Having estimated the efficiency of isocyanate formation, we attempted next to estimate the efficiency of triplet formation. The triplet−triplet UV−vis absorption spectrum of 2-NpCON$_3$ in cyclohexane has been observed previously in conventional laser flash photolysis experiments.[8] The lifetime of the triplet azide is on the order of microseconds[8] in a deoxygenated solvent. Thus, in principle, the 2-NpCON$_3$ triplet state should be detectable by means of fs IR techniques as the residual spectrum recorded 3 ns after the laser excitation. According to calculations at the UB3LYP/TZVP level of theory, the N_3 stretch of triplet 2-NpCON$_3$ is located between the vibrations of the ground and S_1 states (Figure S5, Table S2). On first inspection of the transient spectrum, there is no evidence of a positive band that can be assigned to the triplet azide. However, in two solvents (cyclohexane and carbon tetrachloride), the shape of the transient spectrum recorded at 3 ns does not match the normalized FTIR spectrum (Figure S2a,e), although the concentration of the S_1 state is very low at that time. This difference may be due to triplet formation in these two solvents. In acetonitrile and chloroform, the IR transient spectrum recorded after completion of the S_1 decay has the same shape as the normalized FTIR spectrum (Figures 1 and S2c). If this interpretation is correct, then in acetonitrile and chloroform, the triplet azide must be formed with much lower efficiency than in cyclohexane and carbon tetrachloride.

To estimate the quantum yield of triplet formation for 2-NpCON$_3$ in different solvents (Φ_T, Table S1, Supporting Information, Table 2), the relative actinometry method was applied using transient UV—vis absorption spectroscopy (see Supporting Information for details), and benzophenone was used as the reference compound. In all solvents employed, the transient UV—vis spectra (with a maximum at ~450 nm) were obtained 3 ns after 345 nm laser excitation of 2-NpCON$_3$ (Figure S1, Supporting Information). These spectra are similar to the spectrum assigned previously[8] to the triplet—triplet absorption of 2-NpCON$_3$. The intensity of these spectra was strongly dependent on the solvent polarity and drops significantly upon changing from the nonpolar cyclohexane and CCl$_4$ solvents to more polar solvents. It was assumed that the extinction coefficient at the maximum of the 2-NpCON$_3$ triplet—triplet absorption spectrum in all solvents is the same and is equal to the value of 10500 $L \cdot mol^{-1} \cdot cm^{-1}$ reported for 2-NpCOCH$_3$.[26] The quantum yield of triplet 2-NpCON$_3$ formation is thus estimated to be very low in polar solvents (about 1% in acetonitrile) and relatively high in nonpolar solvents (about 25%, Table S1). Therefore, the concentration of triplet 2-NpCON$_3$ is too low to be detected by fs TRIR spectroscopy in polar solvents.

The absolute rate constants of intersystem crossing ($k_{ISC} = \Phi_T \times \tau^{-1}$) in different solvents can thereby be roughly estimated using values of the triplet quantum yield (Φ_T, Table S1) and the time constants of the S_1 state decay (τ, Table 1). These estimations demonstrate that, within experimental accuracy (~20—30%), the ISC rate constant is independent of the nature of solvent ($k_{ISC} = (3.3 \pm 0.7) \times 10^8$, $(5.1 \pm 1.5) \times 10^8$, $(3.1 \pm 0.9) \times 10^8$, $(2.9 \pm 1.0) \times 10^8$, and $(6 \pm 2) \times 10^8\ s^{-1}$ in cyclohexane, CCl$_4$, CHCl$_3$, CH$_2$Cl$_2$, and CH$_3$CN, respectively).

As the nitrene is not a stable (minutes, hours) photoproduct in solution at room temperature, it was impossible to estimate the efficiency of nitrene formation in different solvents by measuring experimental IR difference spectra. However, the efficiency of nitrene formation ($\Phi_{nitrene}$) was calculated after assuming that ($\Phi_{nitrene} + \Phi_{NCO} + \Phi_T$) = 1. The rate constants of the nitrene formation could then be estimated ($k_{nitrene} = \Phi_{nitrene} \times \tau^{-1}$, Table 2).

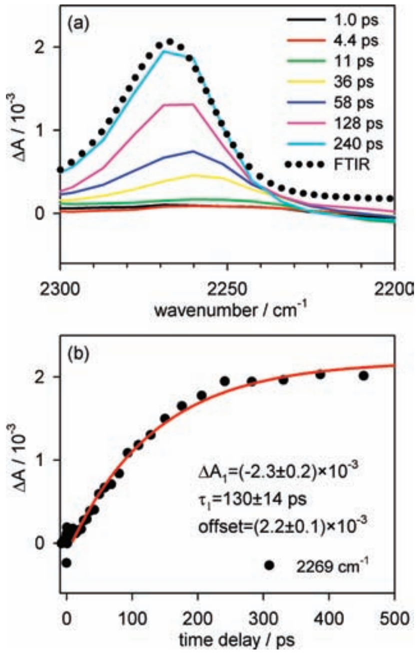

Figure 2. Isocyanate formation from 2-NpCON$_3$ ($c \sim 4.0 \times 10^{-3}$ M) after 350 nm excitation in chloroform. (a) TRIR spectra produced by ultrafast photolysis of 2-NpCON$_3$ in chloroform with 350 nm excitation. The normalized steady-state IR absorption spectrum (FTIR) of 2-NpNCO is also shown as a dotted line. (b) The kinetics of isocyanate formation recorded at 2269 cm^{-1}.

Interestingly, the dependence of the logarithm of the S_1 lifetime on a traditional function of polarity, $f(\varepsilon,n) = (\varepsilon - 1)/(2\varepsilon + 1) - (n^2 - 1)/(2n^2 + 1)$,[24] is linear (Figure S8, Supporting Information). Figure S8 also presents the dependence of the efficiency of isocyanate, nitrene, and triplet formation and the rate constants of these processes versus a function of polarity (data taken from Table 2). Figure S8 clearly shows that the rate constants of isocyanate and nitrene formation increase in polar solvent. The rate constant of the intersystem crossing is almost independent of the solvent polarity. The efficiency of nitrene formation depends slightly on polarity. The efficiency of the isocyanate formation increases significantly as polarity increases, and the opposite trend is observed for the efficiency of triplet formation.

The formation of the isocyanate IR band was studied following 350 nm excitation of 2-NpCON$_3$. The transient spectra recorded in chloroform are shown in Figure 2a. There is a correlation between the rate of decay of the S_1 band and formation of the isocyanate. Both kinetic processes can be adequately described as monoexponential functions. The time constant of the latter process was found to be 130 ± 14 ps (Figure 2b). A global fit of the decay kinetics for the S_1 band and formation kinetics for the isocyanate gave a time constant of 141 ± 6 ps. These results clearly show that the S_1 state of the acyl azide is the precursor of the isocyanate.

A vibrational band of singlet benzoylnitrene has been observed as a doublet at 1727 and 1765 cm^{-1} by matrix isolation spectroscopy (Figure S9, Supporting Information) and in solution at 1760 cm^{-1} by ns IR spectroscopy[5] and by fs IR spectroscopy.[19] On the basis of Autrey and Schuster's[8] product studies, it is clear that nitrene is formed when the S_1 state of 2-NpCON$_3$ is populated by direct excitation with 350 nm light.

Thus, fs TRIR experiments were performed with 340 nm excitation in order to observe nitrene formation in CCl$_4$. The characteristic (cyclic CNO) nitrene band is very weak, but the long decay time constant of the putative precursor S_1 state allows its formation to be monitored. The S_1 lifetime of 2-NpCON$_3$ in CCl$_4$ is about 690 ± 60 ps (Table 1). The transient spectra obtained in CCl$_4$ are shown in Figures 3 and S10, Supporting Information. The intensity of the nitrene band at 1740 cm^{-1} rises with a time

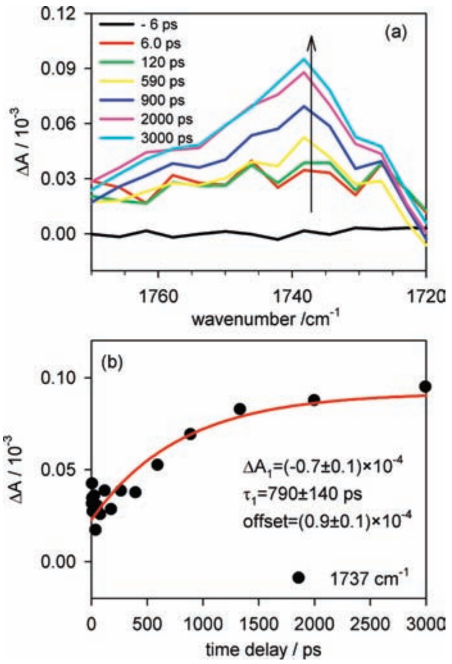

Figure 3. Nitrene formation upon excitation of 2-NpCON$_3$ in carbon tetrachloride ($c \sim 4.0 \times 10^{-3}$ M, λ_{exc} = 340 nm). (a) TRIR spectra produced upon ultrafast photolysis of 2-NpCON$_3$ in CCl$_4$. (b) The kinetics of nitrene formation recorded at 1737 cm^{-1}.

constant of 790 ± 140 ps. This is in fairly good agreement with the time constant of the S$_1$ state decay in this solvent (Table 1). Unfortunately, the accuracy of the time constant measurement is low, as the intensity of the nitrene band is very weak (<10^{-4} OD). Nevertheless, this experiment clearly demonstrates that the acyl azide S$_1$ state is the precursor of nitrene, consistent with the product studies.[8]

A similar pattern of results regarding nitrene formation was observed in CH$_2$Cl$_2$. In this solvent, the S$_1$ state lifetime is equal to 70 ± 6 ps (Table 1). The rise time of the nitrene band in this solvent was found to be 88 ± 14 ps (Figure S11, Supporting Information). These results are significant because in our previous report[19] we were unable to obtain direct kinetic evidence that the S$_1$ state of an acyl azide is the precursor of the corresponding nitrene. However, in our previous studies, the higher electronic states of 2-NpCON$_3$ were populated using 270 nm excitation (vide infra),[19] and the yield of S$_1$ formation from the initially populated S$_n$ ($n \geq 2$) states was low.

Transient UV—Vis Detection. Transient UV—vis absorption spectra were also recorded upon 350 nm excitation of 2-NpCON$_3$ in carbon tetrachloride and in acetonitrile using the pump—probe absorption technique. Excitation of 2-NpCON$_3$ in CCl$_4$ produces a UV—vis transient absorption whose decay is well described by a monoexponential function with a time constant of 425 ± 12 ps (Figure S12, Supporting Information). This time constant is in fair agreement with that measured using the fs TRIR technique (690 ± 60 ps, Table 1). The transient spectrum recorded at ~3 ns is very similar to the triplet—triplet absorption spectrum of Autrey and Schuster as recorded by ns LFP (Figure S13, Supporting Information).[8]

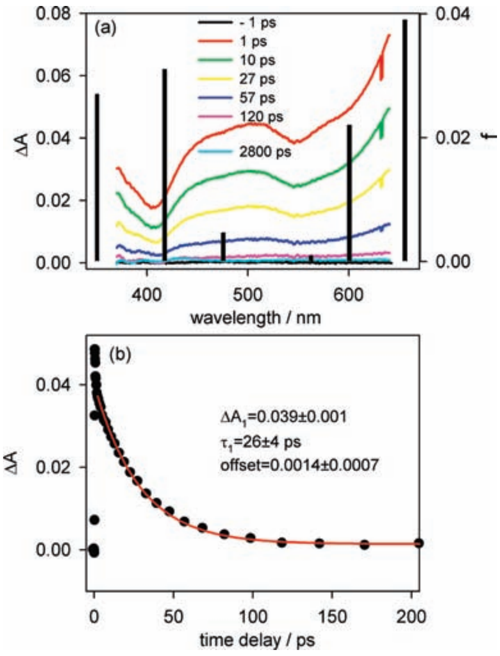

Figure 4. (a) Transient UV—vis spectra produced by fs laser excitation of 2-NpCON$_3$ ($c \sim 4.0 \times 10^{-3}$ M) in acetonitrile (λ_{ex} = 350 nm). The vertical bars indicate the positions and oscillator strengths (f) of the electronic transitions calculated for 2-NpCON$_3$ in the excited singlet (π,π*) state at the MS-CASPT2//CASSCF(14,13) level. (b) Monoexponential fit to the transient absorption kinetics at 500 nm.

As in the case of CCl$_4$, excitation of 2-NpCON$_3$ in acetonitrile yields a UV—vis transient absorption spectrum which decays exponentially with a time constant of 26 ± 4 ps (Figure 4). This time constant is in good agreement with that of the S$_1$ state of 2-NpCON$_3$ obtained by the TRIR technique (28 ± 5 ps, Table 1). In this solvent, the triplet—triplet band was also observed (Figure S14, Supporting Information), but its intensity was very low, which is consistent with the low efficiency of triplet formation in polar solvents (Table 2).

The UV—vis spectrum of 2-NpCON$_3$ in the first singlet excited (π,π*) state has been calculated at the MS-CASPT2//CASSCF level (Figure 4a, Table S4). Calculations predict that this species exhibits strong absorption bands in the visible region. As seen in Figure 4a, the calculated electronic absorption spectrum agrees well with experiment. Note that the experimental transient spectrum may be contaminated in the range of 375—425 nm, due to stimulated emission (Figure S15, Supporting Information). Therefore, calculations support assignment of the transient absorption spectra recorded on the ps time scale (Figures 4 and S12) mainly to 2-NpCON$_3$ in the S$_1$ (π,π*) state.

The results of our ultrafast time-resolved studies with 350 nm excitation light demonstrate that the S$_1$ state of 2-NpCON$_3$ is the precursor of isocyanate and nitrene in all of the solvents employed (Scheme 1). In nonpolar solvents, the triplet state of 2-NpCON$_3$ is also formed in high yield upon direct excitation of the S$_1$ state.

These findings are consistent with prior conclusions based on ns LFP, product studies, and triplet-sensitized experiments, but this is the first direct experimental observation that the decay of the S$_1$ state correlates with the formation of the nitrene. Our results clearly show that internal conversion (S$_1$→S$_0$) and fluorescence are minor processes, as the recovery of the ground state of 2-NpCON$_3$ was not observed up to 3 ns postexcitation. The lifetime of S$_1$ state of 2-NpCON$_3$ is influenced by solvent because the rate constants of the nitrene and isocyanate formation grow significantly as the solvent polarity increases.

Scheme 1

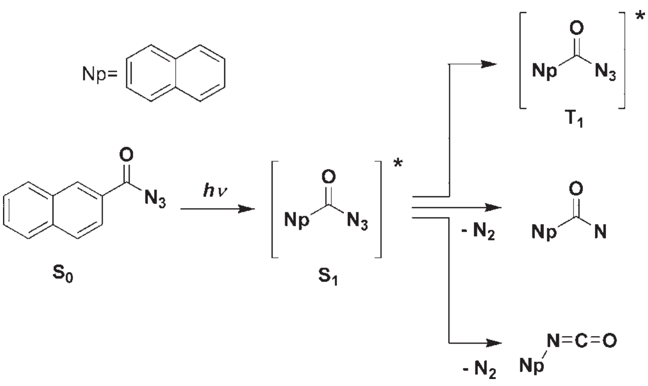

2.2. Ultrafast IR Studies of the 270 nm Photochemistry of 2-NpCON$_3$.

In our communication,[19] the 270 nm photochemistry of 2-NpCON$_3$ in chloroform was studied. Femtosecond time-resolved results obtained with 350 nm excitation for 2-NpCON$_3$ in chloroform can be profitably compared with the data obtained using 270 nm excitation.[19] Similar features were observed in experiments with both excitation wavelengths: two positive bands at 2100 cm^{-1} (S$_1$ state of azide) and at 2265 cm^{-1} (isocyanate), and one negative band at 2140 cm^{-1} (bleaching of azide in the ground state). As the 350 nm light pumps the S$_1$ state directly, the 2100 cm^{-1} band, recorded just after excitation, is much more narrow than that produced with 270 nm light. Clearly, a "hot" S$_1$ state with an initially much broader band is produced with short wavelength light. The time constant of decay of the hot S$_1$ state in chloroform is 6.8 ps (Table 1). Thus, one predicts that the TRIR spectra recorded with 270 nm light, at time delays longer than ~30 ps, should have the same width as the spectra recorded with 350 nm light. Indeed, the transient spectrum recorded at 33 ps using 270 nm excitation has the same shape as the transient spectrum observed at 11 ps with 350 nm excitation (Figure S16, Supporting Information).

To better understand the photochemistry of 2-NpCON$_3$ in higher excited states, experiments in some other solvents were performed. Figures 5 and S17, Supporting Information, present the IR transient absorption spectra produced upon excitation of 2-NpCON$_3$ at 270 nm in selected solvents. With this excitation wavelength, higher electronic states of 2-NpCON$_3$ are immediately populated (vide infra, Table S7). In all solvents employed, 270 nm photoexcitation of 2-NpCON$_3$ yields the 2100 cm^{-1} band, which decays biexponentially. The time constants of this biexponential decay are presented in Table 1.

As in our preliminary report,[19] the fast component (Table 1) was assigned to the hot S$_1$ state of 2-NpCON$_3$ undergoing vibrational relaxation[27,28] and Curtius rearrangement. The slow component was assigned to the decay of the thermally relaxed S$_1$ state of 2-NpCON$_3$. Indeed, the time constants of the slow components obtained with 270 nm excitation are consistent with the time constants obtained when the S$_1$ state was excited directly with 350 nm light.

Although the IR experiments suffer from artifacts[29] in the first picosecond time window, it is very likely that the formation of the 2100 cm^{-1} band is instantaneous (within the laser pulse) in all solvents employed (Figure S18, Supporting Information). Instantaneous growth was also recently observed for benzoyl and pivalolyl azides in chloroform.[19] In all solvents, the maximum of the 2100 cm^{-1} band of 2-NpCON$_3$ shifts to higher frequency by about 5 cm^{-1} (Figure 5, Figure S17). This result is typical of vibrational cooling (VC) in the time window of tens of picoseconds. In nonpolar solvents, this shift is apparently larger. However, this is due to the fact that the low frequency part of this band decays much faster relative to the band of the thermally relaxed S$_1$ state.

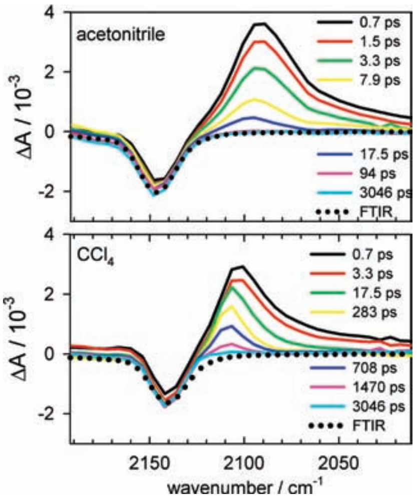

Figure 5. Transient IR spectra produced upon excitation (λ_{exc} = 270 nm) of 2-NpCON$_3$ ($c \sim 1.4 \times 10^{-3}$ M) in acetonitrile and in carbon tetrachloride. The normalized steady state IR absorption spectra (FTIR) of 2-NpCON$_3$ are also shown as dotted lines.

As in the case of 350 nm excitation, there is no recovery of the N$_3$ IR stretch (~2140 cm^{-1}) in the ground state of 2-NpCON$_3$ over 3 ns (Figure S19, Supporting Information). There is only a slight increase of the negative signal at 2140 cm^{-1} due to the overlap of this negative band with the wide, positive 2100 cm^{-1} band (Figures 5, S17, S18, and S19). Recovery of the C=O stretch (~1690 cm^{-1}) in the ground state of 2-NpCON$_3$ was not observed either. Recall that with 350 nm excitation, the weak triplet IR band was detected in CCl$_4$ and cyclohexane (Figure S2a,e). This was also the case when 270 nm excitation was utilized. In these two solvents, the shape of the transient spectrum recorded at 3 ns is clearly different than the appropriately normalized FTIR spectrum (Figures 5 and S17).

In CCl$_4$, the decay of the 2100 cm^{-1} band is slower than that in chloroform,[19] and this allowed us to conveniently monitor the formation of isocyanate band at 2270 cm^{-1} (Figure S20, Supporting Information). The rate of formation of isocyanate is the same as the rate of decay of the 2-NpCON$_3$ in the S$_1$ state (Figure S21, Supporting Information, Table S5), and approximately equal amounts of 2-naphthyl isocyanate are formed in the fast and slow processes.

A similar ratio of the amplitudes of the fast and slow processes was observed in chloroform.[19] These results confirm that both vibrationally hot (S$_1^{\#}$) and cool (S$_1$), first singlet excited states of 2-NpCON$_3$ are precursors of isocyanate. Note, that the isocyanate band recorded immediately after the 270 nm laser excitation in chloroform is shifted to lower frequency relative to the band recorded at longer delays (>30 ps). This is not the case after 350 nm excitation (Figure 2). Thus, formation of the hot isocyanate and its VC were not as prominent with 350 nm irradiation as with 270 nm excitation (Figure S22, Supporting Information).

The fs TRIR results clearly show that the S$_1$ state is a precursor of nitrene when the S$_1$ state is populated directly (350 nm). However,

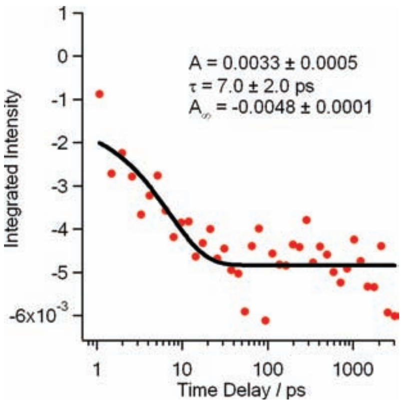

Figure 6. Integrated signal of nitrene band formed upon photolysis of 2-NpCON$_3$ ($c \sim 1.4 \times 10^{-3}$ M) in CCl$_4$ (λ_{exc} = 270 nm).

we were unable to obtain direct evidence for this conclusion using fs TRIR spectroscopy with 270 nm excitation.[19] As the intensity of the nitrene IR band is very low (see Figures 1, S1, and S2 from ref 19 and Figures 3, S10, and S11 in this work) and as VC of the nascent nitrene is relatively slow (30 ps time constant), we could not resolve the dynamics of nitrene formation and could not assign the precursor of singlet 2-NpCON in chloroform[19] when higher electronic states are excited initially with 270 nm light.

Thus, we studied nitrene formation with 2-NpCON$_3$ in CCl$_4$ (λ_{exc} = 270 nm) where the decay of the S$_1$ state is the slowest among the solvents employed and is in fact much slower than that of a typical VC process. The broad band at 1710−1780 cm^{-1} assigned to the singlet nitrene again is formed within the laser pulse. The band sharpens and shifts to higher frequency in about 100 ps (Figure S23, Supporting Information). Note, that there is a difference between the shape of nitrene bands obtained for 2-NpCON$_3$ in CCl$_4$ at 10 ps with two different excitation wavelengths (270 and 340 nm, Figure S24, Supporting Information). With 270 nm excitation, the transient spectrum is more intense and shifted to the lower frequency and thus can be assigned to a hot nitrene. On the other hand, the spectra recorded at 2 ns with both excitations have similar shapes.

The intensity of the nitrene band integrated over the spectral range 1670−1780 cm^{-1} can be fitted to a monoexponential decay curve with a time constant of 7.0 ± 2.0 ps (Figure 6). There is no evidence of a rising component with a time constant close to the lifetime of the thermally equilibrated S$_1$ state of 2-NpCON$_3$ (570 ps in this solvent). Therefore, there is no evidence available from time-resolved IR experiments that some nitrene is formed from the relaxed S$_1$ state of 2-NpCON$_3$, when the precursor is excited at 270 nm in contrast to experiments performed with 340 nm excitation.

Unsurprisingly, the same pattern of results was observed in acetonitrile, a solvent in which the decay of the S$_1$ state is even faster than in chloroform. Yet again, there is no experimental evidence that the formation of the nitrene band correlates (Figure S25, Supporting Information) with the decay of S$_1$ produced indirectly with 270 nm excitation.

To rationalize this conflict, we postulate that with 270 nm excitation, the efficiency of nitrene formation from the upper electronic states (S$_n$, $n \geq 2$) is large, and that the relative yield of nitrene formation from the vibrationally cooled S$_1$ state is small. Thus, formation of the nitrene produced from the relaxed S$_1$ state cannot be resolved from the major pathway because of a low yield superimposed on a larger yielding and faster process. The problem of resolving the minor component of nitrene formation is made more difficult by the intrinsic low amplitude of the nitrene IR band (Figures S10, S11, S23, and S24). As will be shown later, theory supports this explanation (vide infra).

The experiments with 270 and 350 nm excitation were performed using different experimental conditions. To correlate the relative intensities of the S$_1$ band with the excitation wavelength (λ_{exc}), normalization of the transient spectra was performed. The spectra were normalized to the same intensity of the 2140 cm^{-1} bleach of precursor to compare the intensities of the S$_1$ bands produced with different λ_{exc}. Figure S26, Supporting Information, demonstrates that the amplitude of the S$_1$ band recorded with 350 nm light in chloroform is much larger than that recorded with 270 nm light. Note that only ~33% of the signal detected with 270 nm light could be assigned to the thermally relaxed S$_1$ state. As a result, the 2100 cm^{-1} signal detected with 350 nm excitation is about 6 times larger than that for *thermally relaxed S$_1$ state* with 270 nm excitation. Furthermore, if we compare the overall intensity of the 2100 cm^{-1} band in the two experiments, 350 nm excitation leads to about twice the signal strength than production of the corresponding band with 270 nm excitation (Figure S26). This means that only about half of the 2-NpCON$_3$ molecules in the S$_n$ state ($n \geq 2$) produce the S$_1$ state through IC. Similar results were obtained in CCl$_4$ and acetonitrile (Figures S27 and S28, Supporting Information). These results are well explained by the formation of singlet nitrene (2-NpCON) in the upper excited singlet states (S$_n$, $n \geq 2$, Scheme 2).

2.3. Ultrafast UV−Vis Studies of the 270 nm Photochemistry of 2-NpCON$_3$. As 2-NpCON$_3$ has a convenient UV−vis chromophore, fs time-resolved UV−vis transient absorption experiments were also performed in selected solvents: chloroform, acetonitrile, and methanol. In all of the solvents studied, transient spectra were recorded between 350 − 650 nm when 270 nm excitation was utilized. Figure 7 presents the transient absorption spectra detected in chloroform over a −2 to 550 ps time window. A very wide transient absorption spectrum with a maximum at about 470 nm is formed within a laser pulse. This transient absorption decays on a ps time scale. Analysis (Figures S29 and S30, Supporting Information) demonstrates that this decay is best described by a biexponential function with time constants equal to 6 ± 2 and 130 ± 20 ps. These time constants are in very good agreement with the time constants of the azide singlet excited state (S$_1$) decay monitored by fs TRIR techniques (6.8 ± 1.3 and 120 ± 30 ps, Table 1).

The transient spectrum detected 550 ps after the laser pulse has very low intensity ($\Delta A \sim 0.001$). Nevertheless, it is clear that its shape in the range of 400−520 nm is close to that of the triplet−triplet transient absorption spectrum recorded by Autrey and Schuster[8] in cyclohexane at room temperature (Figure S31, Supporting Information).

Note, for singlet benzoylnitrene (PhCON), the transient absorption spectrum has a UV band near 300 nm[5,9] in agreement with TD-B3LYP calculations.[6] A similar spectrum, slightly shifted to the red (~320 nm), was predicted previously[6] for singlet 2-naphthoylnitrene (2-NpCON). Therefore, the singlet nitrene does not contribute noticeably to the experimental transient absorption spectra detected in the range of 380−650 nm (Figure 7).

To determine if excited isocyanate has a contribution to the transient spectra recorded upon excitation of 2-NpCON$_3$, we performed a fs time-resolved UV−vis control study of the isocyanate (2-NpNCO). After excitation of 2-NpNCO with 270 nm light, a wide band was observed, which decays almost to baseline with a time constant of 2.4 ps (Figure S32, Supporting Information).

Scheme 2

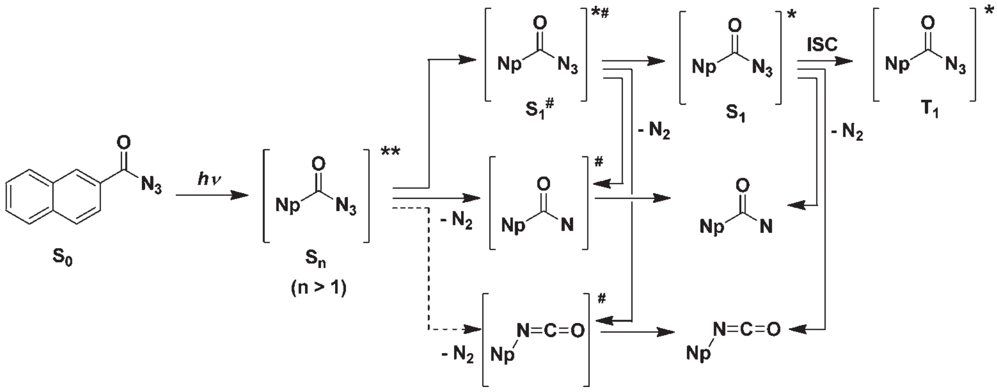

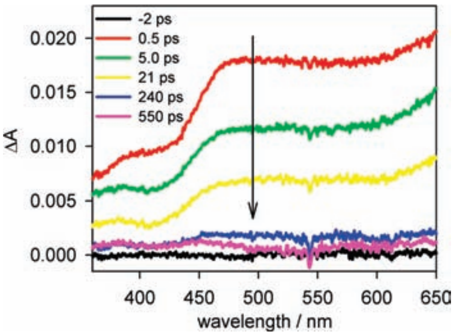

Figure 7. Transient UV−vis absorption spectra obtained upon excitation of 2-NpCON$_3$ ($c \sim 1.4 \times 10^{-3}$ M) in chloroform at ambient temperature recorded at different time delays (λ_{exc} = 270 nm).

Thus, neither the nitrene nor the excited isocyanate contribute to the transient absorption spectra recorded upon excitation of 2-NpCON$_3$. The ground-state isocyanate steady-state absorption spectrum lies below 340 nm (Figure S33, Supporting Information).

A similar pattern of results was observed with 2-NpCON$_3$ in acetonitrile. A very broad transient absorption spectrum is formed within the laser pulse (~300 fs), and then it decays biexponentially (Figures S34, S35, and S36, Supporting Information). Kinetic fits at individual wavelengths (Figure S35) and global analysis (Figure S36) indicate that this decay is best described by a biexponential dependence with time constants equal to 3 ± 1 and 23 ± 4 ps. These time constants are in good agreement with time constants obtained in this solvent by the fs TRIR technique (Table 1). The spectrum detected on a time scale of hundreds of picoseconds has a shape similar (Figure S37, Supporting Information) to the shape of the triplet−triplet absorption of 2-NpCON$_3$ recorded previously in cyclohexane.[8]

Note, in both solvents, the decay-associated spectra (DAS, Figures S30 and S36) corresponding to the fast decay (3 ps in acetonitrile and 6 ps in chloroform) are much wider than the DAS associated with the slow decay (23 and 130 ps, respectively). This confirms that the fast component detected by fs UV−vis spectroscopy is influenced by the band-narrowing effect that is typical of VC.

Thus, in all solvents under study, the same species were detected in both ultrafast IR and UV−vis pump−probe absorption measurements. Excitation of 2-NpCON$_3$ at 270 nm yields a hot first singlet excited state ($S_1^{\#}$) which decays to a thermally equilibrated S$_1$ state with a time constant in the range of 2 to 14 ps depending on the solvent (Table 1). Excitation of 2-NpCON$_3$ at 340 and 350 nm results in the population of the S$_1$ state with only a small excess of vibrational energy, which manifests itself by the absence of the fast decay component. Moreover, in all solvents of this work, the transient absorption UV−vis spectra detected at 3 ns in the range 400−520 nm are in fair agreement with the absorption spectrum detected previously in cyclohexane using conventional LFP techniques and assigned to the triplet−triplet absorption of 2-NpCON$_3$.[8] Note that isocyanate and singlet nitrene have no noticeable absorption in the 350−650 nm spectral region because these species do not absorb light in this spectral range.

3. COMPUTATIONAL RESULTS

Recently, we reported an experimental and computational study of the primary processes in the photochemistry of aryl azides.[30−33] The lifetimes of the singlet excited states of 2-naphthyl azide and 1-chloro-2-naphthyl azide were found to be shorter than 1 ps.[30] A very short lifetime (less than 1 ps) was also observed for excited states of phenyl azide,[32] *p*-biphenyl, *o*-biphenyl, and 1-naphthyl azides.[31,33] According to reported calculations, the detected lifetimes of the excited aryl azides were assigned to the S$_2$ states, rather than the S$_1$ states,[30−33] as the S$_1$ states of the studied aryl azides are dissociative in nature and thus were not detected.

To better understand and support the experimental results obtained in this study, we similarly performed density functional theory calculations on some singlet excited states of 2-NpCON$_3$. In the past, we have shown that the excited state frequencies calculated at the TD-B3LYP/TZVP levels of theory are in very good agreement with the fs TRIR experiments.[34]

Initially, we computed the vertical excitations (Tables S7) for 2-NpCON$_3$ using the optimized ground-state geometry (Tables S8), and then we rendered the corresponding difference density plots in order to identify the character of the singlet excited states (Figures S38, Supporting Information). In order to compute the vibrational spectra of the singlet and triplet excited states, we further optimized the geometries of the excited states (Tables S9' and S10, Supporting Information) using either TD-B3LYP (singlet states) or UB3LYP (triplet states).

A dissociative singlet excited state of the azide unit produces the corresponding singlet nitrene and molecular nitrogen. As was shown for the S$_1$ state of aryl azides, this excitation corresponds to promotion of an electron from the π-orbital of the aryl moiety to the in-plane π* orbital on the azide group. However, as shown

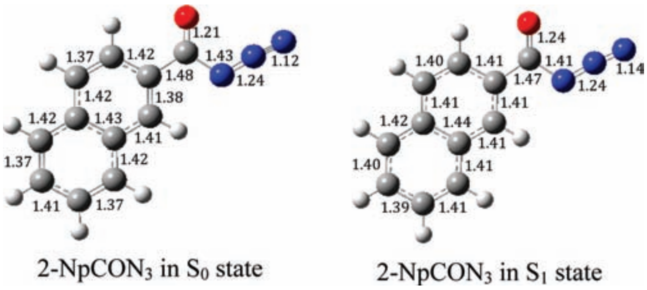

Figure 8. Geometries of the ground (left) and lowest singlet excited (right) states of 2-NpCON$_3$. The ground and S_1 states were optimized at the B3LYP/TZVP and TD-B3LYP/TZVP levels of theory, respectively (bond lengths are in angstroms).

in Figure S38, the S_1 state of 2-NpCON$_3$ is a delocalized (π,π*) excited state, and it does not have significant dissociative character. Nevertheless, it has some electron density accumulation in the π* orbital of the distal N—N bond on the departing N_2 fragment. This aspect would be a significant requirement for a (prompt) dissociative state for nitrene formation from excited carbonyl azides. Indeed, it appears that the "dissociative" state for 2-NpCON$_3$, the S_4 state, is located higher in the singlet manifold.

Femtosecond TRIR experiments demonstrate that upon 270 nm excitation, the nitrene is partly produced by the higher excited singlet states (S_n, $n \geq 2$, Scheme 2). This is in agreement with our computational results, which predict that the S_4 singlet excited state is "dissociative".

Thus, according to theory (see Table S7), the 270 nm laser pulse excites 2-NpCON$_3$ to a "dissociative" excited state where two distinct, concurrent channels were considered: (1) production of the singlet nitrene, and (2) internal conversion to the S_1 state (Scheme 2). This explains why a 270 nm laser pulse simultaneously produces the vibrational band of the nitrene at 1720 cm^{-1} and the 2100 cm^{-1} band belonging to the S_1 excited state of 2-NpCON$_3$. Formation of nitrenes takes place also in the S_1 state, but more slowly and in very low yield, which is evident from the experiments with 350 nm excitation.

In order to support the assignment of the 2100 cm^{-1} experimental band to the S_1 state, we optimized the geometry of the lowest singlet excited state of 2-NpCON$_3$. The optimized geometries of the S_0 and S_1 states of 2-NpCON$_3$ are shown in Figure 8. It is clear from the difference density plots (Figures S38), 2-NpCON$_3$ have an S_1 state that is (π,π*) in nature, and the electronic reorganization is delocalized over the entire molecule. Thus the S_1 state geometries are characterized by changes in the aromatic C=C bond lengths and by only a moderate elongation in the C=O bond length for 2-NpCON$_3$.

The computed frequency of the azide stretch is ~2200 cm^{-1} for the S_1 excited state, which is approximately 100 cm^{-1} higher than the experimental observations. If one applies a scaling factor similar to that used with ground state vibrations, the calculated 2210 cm^{-1} band of the S_1 state of 2-NpCON$_3$ will move to about 2090 cm^{-1} in perfect agreement with the experimentally observed value. Consequently, our calculations support the assignment of the 2100 cm^{-1} band to the S_1 state.

4. CONCLUSIONS

The photochemistry of 2-NpCON$_3$ was studied using ultrafast experimental techniques and computational methods. Excitation of 2-NpCON$_3$ in solvents of different polarity produced a transient IR band at 2100 cm^{-1}. The carrier of the 2100 cm^{-1} transient was assigned to the S_1 state of 2-NpCON$_3$, and this assignment was supported by calculations. Calculations predict that the S_1 state is (π,π*) in nature with the excitation localized mainly on the carbonyl group. However, the frequency of the N_3 stretch in the S_1 state is shifted to lower energy in agreement with experiments. This explains why the S_1 states of carbonyl azides are longer lived and more readily observed than the corresponding S_1 states of aryl azide where the excitation is localized on the azide moiety.

As isocyanates have very strong, characteristic IR bands at about 2260 cm^{-1}, their formation was monitored using the fs IR transient absorption spectroscopy. It was demonstrated that formation of isocyanate (photo-Curtius rearrangement) correlates with the decay of the S_1 singlet excited state of 2-NpCON$_3$ (Scheme 1). Moreover, the photo-Curtius rearrangement proceeds in both the hot and vibrationally cooled S_1 states upon 270 nm excitation (Scheme 2). The hot S_1 state produces isocyanate with a rate constant larger than that of the thermally relaxed S_1 state. When the S_1 state was populated directly using 350 nm excitation, only monoexponential decay of the thermally relaxed S_1 state was observed and the concentration of isocyanate rises monoexponentially as well (Scheme 1). Thus, our experimental results unambiguously demonstrate that isocyanate is produced in the lowest singlet excited state of 2-NpCON$_3$. However, more advanced quantum chemical calculations are required to understand in detail the mechanism of photo-Curtius rearrangement.

It was unambiguously demonstrated that nitrene formation correlates with the S_1 state decay of 2-NpCON$_3$ when the latter is populated by direct excitation with 350 nm light (Scheme 1). This is in accord with the results of product analysis. The singlet nitrene band at 1760 cm^{-1} was also observed upon 270 nm excitation; however, in this case, most of the nitrene is formed instantaneously. Thus, higher singlet excited states of 2-NpCON$_3$ also produce singlet nitrenes (Scheme 2). As the IR markers of the nitrenes near 1760 cm^{-1} are very weak, conclusions based on the IR data cannot be made with certainty. Because 270 nm excitation populates highly excited singlet states (S_n, $n > 1$), it is possible that nitrene is produced from three different azide excited states (Scheme 2): S_n ($n > 1$, very fast process), hot S_1 (fast process), and relaxed S_1 (slow process). According to the calculations, the typical azide dissociative state, similar to those of aryl azides, lies above the S_1 state for 2-NpCON$_3$. This supports our conclusion that the singlet nitrenes are also generated from the highly excited singlet states.

We also found that the bleaching of the IR bands of the ground-state 2-NpCON$_3$ does not recover on the time scale of our experiment (~3 ns). We conclude that internal conversion and fluorescence leading to the ground state of 2-NpCON$_3$ is negligible compared to other deactivation processes in the S_1 state (ISC and isocyanate and nitrene formation).

The graphical scheme of Figure 9 summarizes results of our study and shows different deactivation channels detected for the lowest and upper singlet excited states of 2-NpCON$_3$ using the ultrafast UV—vis and IR spectroscopies.

In contrast to aryl azides, the lifetime of the thermally relaxed S_1 excited state of 2-NpCON$_3$ is relatively long because excitation is localized on the aromatic ring and not directly on the azide group. Moreover, this lifetime depends on the solvent polarity, being shorter in more polar solvents. It was clearly demonstrated that both reactions (isocyanate and nitrene formation) are accelerated by the polar solvent while, as expected, the intersystem crossing rate constant is

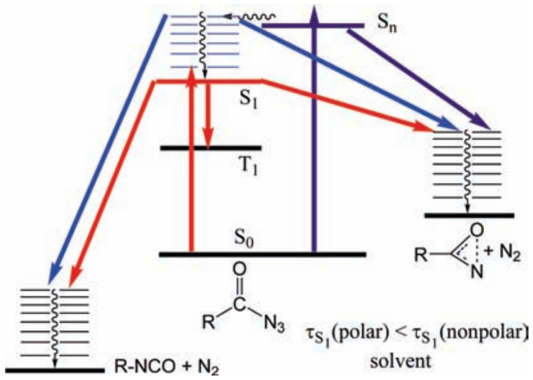

Figure 9. Graphical presentation of the experimental findings.

independent of solvent nature. However, any conclusive mechanistic interpretation of these results awaits more advanced excited-state calculations. To explain the effect of the solvent, extremely rare and computationally expensive calculations need to be carried out to outline the deactivation pathways of the S_1 state in the presence of solvent molecules.

5 . EXPERIMENTAL SECTION

5.1. Materials and Experimental Techniques. Ultrafast IR and UV−vis pump−probe absorption measurements were performed using home-built spectrometers at The Ohio State University. The time resolution is about 300 fs for both the UV−vis and TRIR instruments. They are described in more detail elsewhere.[33,35] Some femtosecond TRIR experiments with 350 nm excitation (time resolution 300 fs) were performed in Lille, France.[23] The absorbance of the sample solutions was about 1.0 in a 1 mm cell at the excitation wavelength. Sample solutions were excited in a stainless steel flow cell equipped with 2 mm thick BaF_2 windows in the case of the IR instrument and CaF_2 windows (1 mm thick front window and 2 mm thick back window) in the case of UV−vis instrument. After passing through the sample, the reference and probe beam were spectrally dispersed with a polychromator and independently imaged on a liquid-nitrogen cooled HgCdTe detector (2 × 32 pixels) (TRIR setup) and thermoelectrically cooled CCD camera (UV−vis setup). The pump pulse energy was $\leq 4\ \mu J$ at the sample position, and the pump beam diameter (fwhm) was equal to about 250 μm. The entire set of pump−probe delay positions (cycle) is repeated at least three times, to observe data reproducibility from cycle to cycle. To avoid rotational diffusion effects, the angle between polarization of the pump beam and the probe beam was set to the magic angle (54.7°). Kinetic traces were analyzed by fitting to a sum of exponential terms. All experiments were performed at room temperature. The relative actinometry method was applied to estimate the quantum yield of triplet formation Φ_T for 2-NpCON$_3$ (Supporting Information).

Acetonitrile, chloroform, and methanol (Burdick and Jackson, spectrometric grade) were used as received. Unless otherwise noted, other materials were obtained from Sigma Aldrich Chemical Co. and used without further purification. The 2-NpCON$_3$ was synthesized following the procedure described for benzoyl azide by Barrett and Porter.[9,36] The 2-naphthyl isocyanate (2-NpNCO) was bought from Aldrich and used as received. Its purity is 97%.

5.2. Computational Methodology. All calculations were performed using the Turbomole-5.91 suite of programs except complete active space (CAS) calculations.[37−39] The ground-state geometry of 2-NpCON$_3$ was optimized at the B3LYP level[40,41] with triple-ζ valence polarized basis sets (TZVP),[42] using C_1 symmetry. Vertical excitations were computed using the time-dependent (TD) B3LYP[43] level of theory at these ground-state geometries. To characterize the excited states, we computed difference electronic density plots (between S_0 and S_1−S_4 states) as described in previous reports.[44−46] The first singlet excited state of 2-NpCON$_3$ was optimized at the TD-B3LYP/TZVP level of theory. The stationary point obtained for the singlet excited state was confirmed to be a minimum by calculating the second derivatives numerically, utilizing the NumForce module in Turbomole, thereby also predicting the infrared (IR) spectrum of the excited state at the TD-B3LYP/TZVP level of theory.

Vertical excitation energies of 2-NpCON$_3$ in the first excited singlet state were calculated at the TD-B3LYP/TZVP geometry (Table S9) by the MS-CASPT2//CASSCF procedure[47] with the ANO-S basis set of Pierloot et al.[48] using the MOLCAS program[49] under limiting conditions of C_s symmetry. In order to arrive at a satisfactory description of all excited states at the CASPT2 level (i.e., to remove intruder states), the imaginary level-shifting technique was used.[50] The active space used in these calculations included 14 electrons with 13 orbitals (Figure S39, Supporting Information).

■ ASSOCIATED CONTENT

Ⓢ **Supporting Information.** Spectra and kinetics of ultrafast studies, the quantum yields of triplet formation (Φ_T) for 2-NpCON$_3$ in different solvents, and details of the quantum chemical calculations. This material is available free of charge via the Internet at http://pubs.acs.org.

■ AUTHOR INFORMATION

Corresponding Author

hadad.1@osu.edu; platz.1@osu.edu

Present Addresses

[#]Department of Chemistry, 101 South Rd., The University of North Carolina, Chapel Hill, NC 27514.

■ ACKNOWLEDGMENT

This work was performed at The Ohio State University Center for Chemical and Biophysical Dynamics. Support by the National Science Foundation is gratefully acknowledged along with generous allocations of computational resources by the Ohio Supercomputer Center. M.S. acknowledge funding from the French Centre Nationale de la Recherche Scientifique (CNRS), the Ministère de l'Enseignement Supérieur et de la Recherche and the Région Nord-Pas de Calais. S.V. gratefully acknowledges an Ohio State University Presidential Fellowship.

■ REFERENCES

(1) Platz, M. S. *Nitrenes in Reactive Intermediate Chemistry*; Moss, R. A.; Platz, M. S.; Jons, M. J., Eds.; John Wiley & Sons, Inc.: Hoboken, NJ, 2005; pp 501−559.

(2) Gritsan, N. P. *Russ. Chem. Rev.* **2007**, *76*, 1139.

(3) Bayley, H.; Staros, J. *Azides and Nitrenes; Reactivity and Utility*; Scriven, E.F.V., Ed.; Academic Press: New York, 1984.

(4) Gritsan, N. P.; Platz, M. S. *Chem. Rev.* **2006**, *106*, 3844.

(5) Pritchina, E. A.; Gritsan, N. P.; Maltsev, A.; Bally, T.; Autrey, T.; Liu, Y.; Wang, Y.; Toscano, J. P. *Phys. Chem. Chem. Phys.* **2003**, *5*, 1010.

(6) Gritsan, N. P.; Pritchina, E. A. *Mendeleev Commun.* **2001**, *11*, 94.

(7) Sigman, M. E.; Autrey, T.; Schuster, G. B. *J. Am. Chem. Soc.* **1988**, *110*, 4297.

(8) Autrey, T.; Schuster, G. B. *J. Am. Chem. Soc.* **1987**, *109*, 5814.

(9) Liu, J.; Mandel, S.; Hadad, C. M.; Platz, M. S. *J. Org. Chem.* **2004**, *69*, 8583.

(10) McCulla, R. D.; Gohar, G. A.; Hadad, C. M.; Platz, M. S. *J. Org. Chem.* **2007**, *72*, 9426.

(11) Caraculacu, A. A.; Coseri, S. *Prog. Polym. Sci.* **2001**, *26*, 799.

(12) Wentrup, C.; Bornemann, H. *Eur. J. Org. Chem.* **2005**, *2005* 4521.

(13) Linke, S.; Tisue, G. T.; Lwowski, W. *J. Am. Chem. Soc.* **1967**, *89* 6308.

(14) Tisue, G. T.; Linke, S.; Lwowski, W. *J. Am. Chem. Soc.* **1967**, *89* 6303.

(15) Lwowski, W.; Tisue, G. T. *J. Am. Chem. Soc.* **1965**, *87*, 4022.

(16) Zabalov, M.; Tiger, R. *Russ. Chem. Bull.* **2005**, *54*, 2270.

(17) Eibler, E.; Sauer, J. *Tetrahedron Lett.* **1974**, *15*, 2569.

(18) Semenov, V. P.; Studenikov, A. N.; Bespalov, A. D.; Ogloblin, K. A. *Zh. Organ. Khim. (Russ.)* **1977**, *13*, 2202.

(19) Kubicki, J.; Zhang, Y.; Wang, J.; Luk, H. L.; Peng, H.-L.; Vyas, S.; Platz, M. S. *J. Am. Chem. Soc.* **2009**, *131*, 4212.

(20) Bonneau, R.; Liu, M. T. H.; Kim, K. C.; Goodman, J. L. *J. Am. Chem. Soc.* **1996**, *118*, 3829.

(21) Desikan, V.; Liu, Y.; Toscano, J. P.; Jenks, W. S. *J. Org. Chem.* **2007**, *72*, 6848.

(22) Desikan, V.; Liu, Y.; Toscano, J. P.; Jenks, W. S. *J. Org. Chem.* **2008**, *73*, 4398.

(23) Zhang, Y.; Burdzinski, G.; Kubicki, J.; Vyas, S.; Hadad, C. M.; Sliwa, M.; Poizat, O.; Buntinx, G.; Platz, M. S. *J. Am. Chem. Soc.* **2009**, *131*, 13784.

(24) Suppan, P.; Ghoneim, N. *Solvatochromism*; The Royal Society of Chemistry, Cambridge, 1997.

(25) Nibbering, E. T. J.; Elsaesser, T. *Appl. Phys. B: Lasers Opt.* **2000**, *71*, 439.

(26) Carmichael, I.; Hug, G. L. *J. Phys. Chem. Ref. Data* **1986**, *15*, 1.

(27) Klessinger, M.; Michl, J. In *Excited States and Photochemistry of Organic Molecules*; VCH Publishers, Inc.: New York, 1995; Chapter 6. Photochemical Reaction Model. 309−360.

(28) Rabinovitch, B. S.; Rynbrandt, J. D. *J. Phys. Chem.* **1971**, *75*, 2164.

(29) Hamm, P. *Chem. Phys.* **1995**, *200*, 415.

(30) Wang, J.; Kubicki, J.; Burdzinski, G.; Hackett, J. C.; Gustafson, T. L.; Hadad, C. M.; Platz, M. S. *J. Org. Chem.* **2007**, *72*, 7581.

(31) Wang, J.; Burdzinski, G.; Zhu, Z.; Platz, M. S.; Carra, C.; Bally, T. *J. Am. Chem. Soc.* **2007**, *129*, 8380.

(32) Wang, J.; Kubicki, J.; Platz, M. S. *Org. Lett.* **2007**, *9*, 3973.

(33) Burdzinski, G.; Hackett, J. C.; Wang, J.; Gustafson, T. L.; Hadad, C. M.; Platz, M. S. *J. Am. Chem. Soc.* **2006**, *128*, 13402.

(34) Li, G.; Parimal, K.; Vyas, S.; Hadad, C. M.; Flood, A. H.; Glusac, K. D. *J. Am. Chem. Soc.* **2009**, *131*, 11656.

(35) Wang, J.; Burdzinski, G.; Kubicki, J.; Platz, M. S. *J. Am. Chem. Soc.* **2008**, *130*, 11195.

(36) Barrett, E. W.; Porter, C. W. *J. Am. Chem. Soc.* **1941**, *63*, 3434.

(37) Treutler, O.; Ahlrichs, R. *J. Chem. Phys.* **1995**, *102*, 346.

(38) Ahlrichs, R.; Bär, M.; Häser, M.; Horn, H.; Kölmel, C. *Chem. Phys. Lett.* **1989**, *162*, 165.

(39) For the current version of TURBOMOLE, see http://www.turbomole.de.

(40) Becke, A. D. *J. Chem. Phys.* **1993**, *98*, 5648.

(41) Lee, C.; Yang, W.; Parr, R. G. *Phys. Rev. B* **1988**, *37*, 785.

(42) Weigend, F.; Häser, M.; Patzelt, H.; Ahlrichs, R. *Chem. Phys. Lett.* **1998**, *294*, 143.

(43) Olivucci, M. *Computational Photochemistry*; Elsevier: Amsterdam, 2005.

(44) Vyas, S.; Onchoke, K. K.; Rajesh, C. S.; Hadad, C. M.; Dutta, P. K. *J. Phys. Chem. A* **2009**, *113*, 12558.

(45) Vyas, S.; Hadad, C. M.; Modarelli, D. A. *J. Phys. Chem. A* **2008**, *112*, 6533.

(46) Burdzinski, G. T.; Gustafson, T. L.; Hackett, J. C.; Hadad, C. M.; Platz, M. S. *J. Am. Chem. Soc.* **2005**, *127*, 13764.

(47) Finley, J.; Malmqvist, P.-Ĺ.; Roos, B. O.; Serrano-Andrés, L. *Chem. Phys. Lett.* **1998**, *288*, 299.

(48) Pierloot, K.; Dumez, B.; Widmark, P.-O.; Roos, B. O. *Theor. Chim. Acta* **1995**, *90*, 87.

(49) Karlström, G.; Lindh, R.; Malmqvist, P.-Ĺ.; Roos, B. O.; Ryde, U.; Veryazov, V.; Widmark, P.-O.; Cossi, M.; Schimmelpfennig, B.; Neogrady, P.; Seijo, L. *Comput. Mater. Sci.* **2003**, *28*, 222.

(50) Forsberg, N.; Malmqvist, P.-Ĺ. *Chem. Phys. Lett.* **1997**, *274*, 196.